

NONLINEAR DYNAMICS OF THE 3D PENDULUM*

NALIN A. CHATURVEDI[†], TAEYOUNG LEE[‡], MELVIN LEOK[§], AND N. HARRIS MCCLAMROCH[¶]

Abstract. A 3D pendulum consists of a rigid body, supported at a fixed pivot, with three rotational degrees of freedom. The pendulum is acted on by a gravitational force. Symmetry assumptions are shown to lead to the planar 1D pendulum and to the spherical 2D pendulum models as special cases. The case where the rigid body is asymmetric and the center of mass is distinct from the pivot location leads to the 3D pendulum. Full and reduced 3D pendulum models are introduced and used to study important features of the nonlinear dynamics: conserved quantities, equilibria, invariant manifolds, local dynamics near equilibria and invariant manifolds, and the presence of chaotic motions. These results demonstrate the rich and complex dynamics of the 3D pendulum.

Key words. Pendulum, rigid body, nonlinear dynamics, attitude, equilibria, stability, chaos

AMS subject classifications. 70E17, 70K20, 70K42, 65P20

1. Introduction. Pendulum models have been a rich source of examples in nonlinear dynamics and in recent decades, in nonlinear control. The most common rigid pendulum model consists of a mass particle that is attached to one end of a massless, rigid link; the other end of the link is fixed to a pivot point that provides a rotational joint for the link and mass particle. If the link and mass particle are constrained to move within a fixed plane, the system is referred to as a planar 1D pendulum. If the link and mass particle are unconstrained, the system is referred to as a spherical 2D pendulum. Planar and spherical pendulum models have been studied in [10, 1].

Numerous extensions of simple pendulum models have been proposed. These include various categories of elastic pendulum models and multi-body pendulum models. Interesting examples of multi-body pendulum models are: a pendulum on a cart, an acrobot, a pendubot, a pendulum actuated by a reaction wheel, the Furuta pendulum, and pendula consisting of multiple coupled bodies.

Pendulum models are useful for both pedagogical and research reasons. They represent physical mechanisms that can be viewed as simplified academic versions of mechanical systems that arise, for example, in robotics and spacecraft. In addition to their important role in illustrating the fundamental techniques of nonlinear dynamics, pendulum models have motivated new research directions and applications in nonlinear dynamics.

This paper considers a new 3D pendulum model, first introduced in [16], and analyzes its nonlinear dynamical properties. This model consists of a rigid body, supported at a fixed pivot point that has three rotational degrees of freedom; it is acted on by a uniform gravity force. Control and disturbance forces and moments are ignored in this development.

This paper arose out of our continuing research on a laboratory facility, referred to as the Triaxial Attitude Control Testbed (TACT). The TACT has been constructed to provide a testbed for a variety of physical experiments on attitude dynamics and attitude control. The most important feature of the TACT design is that it is supported by a three-dimensional air bearing that serves as an ideal frictionless pivot, allowing nearly unrestricted three degrees of rotation. The TACT has been described in several prior conference publications [4, 9]. Issues of nonlinear dynamics for the TACT have been treated in [9, 8]. The present paper is partly motivated by the realization that the TACT is, in fact, a physical implementation of a 3D pendulum.

2. Description of the 3D Pendulum. A rigid 3D pendulum is a rigid body supported by a fixed, frictionless pivot, acted on by gravitational forces. The supporting pivot allows the pendulum three rotational degrees of freedom. Uniform, constant gravity is assumed. The terminology 3D pendulum refers to the fact

*NC, TL and NHM have been supported in part by NSF Grant ECS-0244977 and CMS-0555797. TL and ML have been supported in part by NSF Grant DMS-0504747 and DMS-0726263.

[†]Department of Aerospace Engineering, The University of Michigan, Ann Arbor, Michigan 48109-2140 (nalin@umich.edu).

[‡]Department of Aerospace Engineering, The University of Michigan, Ann Arbor, Michigan 48109-2140 (tylee@umich.edu).

[§]Department of Mathematics, Purdue University, West Lafayette, IN 47907-2067 (mleok@math.purdue.edu).

[¶]Department of Aerospace Engineering, The University of Michigan, Ann Arbor, Michigan 48109-2140 (nhm@umich.edu).

that the pendulum is a rigid body with three spatial dimensions and the pendulum has three rotational degrees of freedom.

Two reference frames are introduced. An inertial reference frame has its origin at the pivot; the first two axes lie in the horizontal plane and the third axis is vertical in the direction of gravity. A reference frame fixed to the pendulum body is also introduced. The origin of this body-fixed frame is also located at the pivot. In the body fixed frame, the moment of inertia of the pendulum is constant. This moment of inertia can be computed using the parallel axis theorem from the traditional moment of inertia with respect to a translated frame whose origin is located at the center of mass of the pendulum. Since the origin of the body fixed frame is located at the pivot, principal axes with respect to this frame can be defined for which the moment of inertia is a diagonal matrix. Note that the center of mass of the 3D pendulum may or may not lie on one of the principal axes defined in this way.

Rotation matrices can be used to describe the attitude of the rigid 3D pendulum. A rotation matrix maps a representation of vectors expressed in the body-fixed frame to a representation expressed in the inertial frame. Rotation matrices provide global representations of the attitude of the pendulum, which is why they are utilized here. Other attitude representations, such as exponential coordinates, quaternions, or Euler angles, can also be used following standard descriptions, but each of the representations has a disadvantage of introducing an ambiguity or singularity. In this paper, the configuration of the rigid pendulum is a rotation matrix R in the special orthogonal group $SO(3)$ defined as

$$SO(3) \triangleq \{R \in \mathbb{R}^{3 \times 3} : RR^T = I_{3 \times 3}, \det(R) = 1\}.$$

The associated angular velocity, expressed in the body-fixed frame, is denoted by $\omega \in \mathbb{R}^3$. The constant inertia matrix, in the body-fixed frame, is denoted by the symbol J . The constant body-fixed vector from the pivot to the center of mass of the pendulum is denoted by ρ . The symbol g denotes the constant acceleration due to gravity.

Three categories of 3D pendulum models are subsequently introduced and studied. The “full” dynamics of the 3D pendulum are based on Euler’s equations that include the gravity moment and the rotational kinematics, expressed in terms of the angular velocity and a rotation matrix; this model describes the dynamics that evolves on $TSO(3)$. Since the gravity moment depends solely on the direction of gravity in the pendulum fixed frame, it is possible to obtain a reduced model expressed in terms of the angular velocity and a unit vector that defines the direction of gravity in the pendulum fixed frame; this model describes the dynamics that evolve on $TSO(3)/S^1$, and corresponds to the case of Lagrange–Poincaré reduction [6]. Since there is a symmetry action given by a rotation about the gravity direction, Lagrange–Routh reduction [15] leads to a reduced model that is restricted to a constant momentum surface and is expressed in terms of the unit vector that defines the direction of gravity in the pendulum fixed frame and its derivative; this model describes the dynamics that evolve on TS^2 . Each of these 3D pendulum models provides special insight into the nonlinear dynamics. We develop each of these models in this paper, and we investigate the features of the nonlinear dynamics, namely invariants, equilibria, and stability for each model.

3. 3D Pendulum Dynamics on $TSO(3)$. The dynamics of the 3D pendulum are given by the Euler equation that includes the moment due to gravity:

$$J\dot{\omega} = J\omega \times \omega + mg\rho \times R^T e_3. \quad (3.1)$$

The rotational kinematics equations are

$$\dot{R} = R\hat{\omega}. \quad (3.2)$$

Equations (3.1) and (3.2) define the full dynamics of a rigid pendulum on the tangent bundle $TSO(3)$. In the above equations, $e_3 = (0, 0, 1)^T$ is the direction of gravity in the inertial frame, so that $R^T e_3$ is the direction of gravity in the pendulum-fixed frame. The cross product notation $a \times b$ for vectors $a, b \in \mathbb{R}^3$ is

$$a \times b = [a_2 b_3 - a_3 b_2, a_3 b_1 - a_1 b_3, a_1 b_2 - a_2 b_1] = \hat{a}b, \quad (3.3)$$

where, the skew-symmetric matrix \hat{a} is defined as

$$\hat{a} = \begin{bmatrix} 0 & -a_3 & a_2 \\ a_3 & 0 & -a_1 \\ -a_2 & a_1 & 0 \end{bmatrix}. \quad (3.4)$$

A special case occurs if the center of mass of the rigid pendulum is located at the pivot. In this case $\rho = 0$, so that (3.1) is given by Euler's equations with no gravity terms included. In the context of the rigid 3D pendulum, this is referred to as the balanced case. Since there is a large literature on Euler's equations with no gravity moment and the associated rotational kinematics, this case is not considered further in this paper. Rather, the focus of this paper is on the unbalanced case, where $\rho \neq 0$.

3.1. Invariants of the 3D Pendulum. There are two conserved quantities for the rigid 3D pendulum. First, the total energy, which is the sum of the rotational kinetic energy and the gravitational potential energy, is conserved. In addition, there is a symmetry corresponding to rotations about the gravity direction through the pivot. This symmetry leads to conservation of the component of angular momentum about the gravity direction. These two results are summarized as follows.

Proposition 1. *The total energy*

$$E = \frac{1}{2} \omega^T J \omega - mg \rho^T R^T e_3,$$

and the component of the angular momentum vector about the vertical axis through the pivot

$$h = \omega^T J R^T e_3.$$

are each constant along motions of the rigid 3D pendulum.

Proof. The proof follows by showing that the time derivative of the total energy and the time derivative of the angular momentum component about the vertical axis are each identically zero. We use (3.1) and (3.2) to compute the derivatives, yielding

$$\dot{E} = \omega^T J \dot{\omega} - mg \rho^T \dot{R}^T e_3 = mg \omega^T (\rho \times R^T e_3) + mg \rho^T (\omega \times R^T e_3) = 0,$$

and similarly,

$$\begin{aligned} \dot{h} &= \dot{\omega}^T J R^T e_3 + \omega^T J \dot{R}^T e_3, \\ &= (J \omega \times \omega)^T (R^T e_3) + (mg \rho \times R^T e_3)^T (R^T e_3) - \omega^T J (\omega \times R^T e_3), \\ &= (J \omega)^T (\omega \times R^T e_3) - \omega^T J (\omega \times R^T e_3) = 0. \end{aligned}$$

□

Conservation of the angular momentum component about the vertical axis will be revisited in Section 5 in the context of Noether's theorem, which states that the momentum map associated with the rotational symmetry about the gravity direction is conserved.

3.2. Equilibria of the 3D Pendulum. To further understand the dynamics of the 3D pendulum, we study its equilibria. Equating the RHS of (3.1) and (3.2) to zero yields

$$J \omega_e \times \omega_e + mg \rho \times R_e^T e_3 = 0, \quad (3.5)$$

$$R_e \hat{\omega}_e = 0. \quad (3.6)$$

Since $R_e \in SO(3)$ is non-singular, and $\hat{\cdot}: \mathbb{R}^3 \rightarrow \mathbb{R}^{3 \times 3}$ is a linear injection, $R_e \hat{\omega}_e = 0$ if and only if $\omega_e = 0$. Substituting $\omega_e = 0$ in (3.5), we obtain

$$\rho \times R_e^T e_3 = 0. \quad (3.7)$$

Hence,

$$R_e^T e_3 = \frac{\rho}{\|\rho\|}, \quad (3.8)$$

or

$$R_e^T e_3 = -\frac{\rho}{\|\rho\|}. \quad (3.9)$$

An attitude R_e is an equilibrium attitude if and only if the direction of gravity resolved in the body-fixed frame, $R_e^T e_3$, is collinear with the vector ρ . If $R_e^T e_3$ is in the same direction as the vector ρ , then $(R_e, 0)$ is a *hanging equilibrium* of the 3D pendulum; if $R_e^T e_3$ is in the opposite direction as the vector ρ , then $(R_e, 0)$ is an *inverted equilibrium* of the 3D pendulum.

Thus, if R_e defines an equilibrium attitude for the 3D pendulum, then a rotation of the 3D pendulum about the gravity vector by an arbitrary angle is also an equilibrium. Consequently, in $TSO(3)$ there are two disjoint equilibrium manifolds of the 3D pendulum. The manifold corresponding to the first case in the above description is referred to as the hanging equilibrium manifold, since the center of mass is below the pivot for each attitude in the manifold. The manifold corresponding to the second case in the above description is referred to as the inverted equilibrium manifold, since the center of mass is above the pivot for each attitude in the manifold.

Following (3.8) and (3.9) and the discussion above, we define

$$[R]_h \triangleq \left\{ R \in SO(3) : R^T e_3 = \frac{\rho}{\|\rho\|} \right\}, \quad (3.10)$$

$$[R]_i \triangleq \left\{ R \in SO(3) : R^T e_3 = -\frac{\rho}{\|\rho\|} \right\}, \quad (3.11)$$

as the *hanging attitude manifold* and the *inverted attitude manifold*, respectively.

From (3.8) and (3.9),

$$\mathbb{H} \triangleq \left\{ (R, 0) \in TSO(3) : R \in [R]_h \right\}, \quad (3.12)$$

is the manifold of hanging equilibria and

$$\mathbb{I} \triangleq \left\{ (R, 0) \in TSO(3) : R \in [R]_i \right\}, \quad (3.13)$$

is the manifold of inverted equilibria, and these two equilibrium manifolds are clearly distinct.

3.3. Local Analysis of the 3D Pendulum near an Equilibrium. Consider a perturbation of the initial conditions from a hanging equilibrium $(R_e, 0)$ of the 3D pendulum, using a perturbation parameter ε . Let $R^\varepsilon(t)$ and $\omega^\varepsilon(t)$ represent the perturbed solution, corresponding to initial conditions $R^\varepsilon(0) = R_e \exp \varepsilon \widehat{\delta\Theta}$ and $\omega^\varepsilon(0) = \varepsilon \delta\omega$, where $\delta\Theta, \delta\omega \in \mathbb{R}^3$ are constant vectors. Note that if $\varepsilon = 0$ then, $(R^0(0), \omega^0(0)) = (R_e, 0)$ and hence

$$(R^0(t), \omega^0(t)) \equiv (R_e, 0) \quad (3.14)$$

for all time $t \in \mathbb{R}$, which simply corresponds to the unperturbed equilibrium solution.

Consider the solution to the perturbed equations of motion for the 3D pendulum. This solution satisfies

$$J\dot{\omega}^\varepsilon = J\omega^\varepsilon \times \omega^\varepsilon + mg\rho \times (R^\varepsilon)^T e_3, \quad (3.15)$$

$$\dot{R}^\varepsilon = R^\varepsilon(t) \widehat{\omega}^\varepsilon. \quad (3.16)$$

Next, we differentiate both sides with respect to ε and substitute $\varepsilon = 0$, yielding

$$J\dot{\omega}_\varepsilon^0 = J\omega_\varepsilon^0 \times \omega^0 + J\omega^0 \times \omega_\varepsilon^0 + mg\rho \times (R_\varepsilon^0)^T e_3, \quad (3.17)$$

$$\dot{R}_\varepsilon^0 = R_\varepsilon^0 \widehat{\omega}_\varepsilon^0 + R^0 \widehat{\omega}_\varepsilon^0, \quad (3.18)$$

where the subscripts denote derivatives. Substituting $R^0 = R_e$ and $\omega^0 = 0$ from (3.14) into (3.17) and (3.18) yields

$$J\dot{\omega}_\varepsilon^0 = mg\rho \times (R_\varepsilon^0)^\top e_3, \quad (3.19)$$

$$\dot{R}_\varepsilon^0 = R_e \hat{\omega}_\varepsilon^0. \quad (3.20)$$

Now we define perturbation variables $\Delta\omega(t) \triangleq \omega_\varepsilon^0(t)$ and $\widehat{\Delta\Theta}(t) \triangleq R_e^\top R_\varepsilon^0(t)$. It can be shown that $\Delta\omega(t) = \Delta\dot{\Theta}(t)$. Thus, (3.19) and (3.20) can be written as

$$J\Delta\ddot{\Theta} - \frac{mg\hat{\rho}^2}{\|\rho\|}\Delta\Theta = 0. \quad (3.21)$$

Note that (3.21) represents a mechanical system with mass matrix J , stiffness matrix $-\frac{mg\hat{\rho}^2}{\|\rho\|}$, but no damping. Since $\hat{\rho}^2$ is a negative-semidefinite matrix with two negative eigenvalues and one zero eigenvalue, the stiffness matrix is positive-semidefinite with two positive eigenvalues and one zero eigenvalue. The zero eigenvalue corresponds to rotations about the vertical axis, for which gravity has no influence. To see this more explicitly, we next perform a transformation of variables.

As $\hat{\rho}^2$ is a rank 2, symmetric, negative-semidefinite matrix, it follows from [2, 3] that one can simultaneously diagonalize J and $\hat{\rho}^2$. Thus, there exists a non-singular matrix M such that $J = MM^\top$ and $-\frac{mg}{\|\rho\|}\hat{\rho}^2 = M\Lambda M^\top$, where Λ is a diagonal matrix. Let $\Lambda = \text{diag}(mgl_1, mgl_2, 0)$, where l_1 and l_2 are positive. Define $x \triangleq M^\top \Delta\Theta$. Then expressing $x = (x_1, x_2, x_3) \in \mathbb{R}^3$, equation (3.21) can be written as

$$\ddot{x}_1 + mgl_1 x_1 = 0, \quad (3.22)$$

$$\ddot{x}_2 + mgl_2 x_2 = 0, \quad (3.23)$$

$$\ddot{x}_3 = 0. \quad (3.24)$$

Thus, the variable x_3 represents a perturbation in attitude of the 3D pendulum that corresponds to a rotation about the vertical axis.

Due to the presence of imaginary and zero eigenvalues of the linearized equations, no conclusion can be made about the stability of the hanging equilibrium or the hanging equilibrium manifold of the 3D pendulum. Indeed, the local structure of trajectories in an open neighborhood the equilibrium is that of a center manifold; there are no stable or unstable manifolds. We next show that the hanging equilibrium manifold of the 3D pendulum is Lyapunov stable.

Proposition 2. *Consider the 3D pendulum model described by equations (3.1) and (3.2). Then, the hanging equilibrium manifold \mathbf{H} given by (3.12) is stable in the sense of Lyapunov.*

Proof. Consider the following positive-semidefinite function on $TSO(3)$

$$V(R, \omega) = \frac{1}{2} \omega^\top J \omega + mg(\|\rho\| - \rho^\top R^\top e_3). \quad (3.25)$$

Note that $V(R, 0) = 0$ for all $(R, \omega) \in \mathbf{H}$ and $V(R, \omega) > 0$ elsewhere. Furthermore, the derivative along a solution of (3.1) and (3.2) is given by

$$\begin{aligned} \dot{V}(R, \omega) &= \omega^\top J \dot{\omega} - mg\rho^\top \dot{R}^\top e_3, \\ &= \omega^\top (J\omega \times \omega + mg\rho \times R^\top e_3) - mg\rho^\top (-\hat{\omega}R^\top e_3), \\ &= mg \left[\omega^\top (\rho \times R^\top e_3) + \rho^\top (\omega \times R^\top e_3) \right] = 0. \end{aligned}$$

Thus, \dot{V} is negative-semidefinite on $TSO(3)$. Also, every sublevel set of the function V is compact. Therefore, the hanging equilibrium manifold \mathbf{H} is Lyapunov stable. \square

Similarly, one can linearize the 3D pendulum dynamics about an equilibrium in the inverted equilibrium manifold. Expressing this linearization in terms of $(x_1, x_2, x_3) \in \mathbb{R}^3$ as in (3.22)–(3.24), it can be shown that the linearization of the 3D pendulum about an inverted equilibrium can be written as

$$\ddot{x}_1 - mgl_1x_1 = 0, \quad (3.26)$$

$$\ddot{x}_2 - mgl_2x_2 = 0, \quad (3.27)$$

$$\ddot{x}_3 = 0. \quad (3.28)$$

The linearization of the 3D pendulum about an inverted equilibrium results in a system that has two positive eigenvalues, two negative eigenvalues and two zero eigenvalues. Thus, the inverted equilibrium has a two dimensional stable manifold, a two dimensional unstable manifold and a two dimensional center manifold. It is clear that due to the presence of the two positive eigenvalues, the inverted equilibrium is unstable.

Proposition 3. *Consider the 3D pendulum model described by equations (3.1) and (3.2). Then, each equilibrium in the inverted equilibrium manifold \mathbf{I} given by (3.13) is unstable.*

4. Lagrange–Poincaré Reduced 3D Pendulum Dynamics on $TSO(3)/S^1$. The equations of motion (3.1) and (3.2) for the 3D pendulum are viewed as a model for the dynamics on the tangent bundle $TSO(3)$ [5]; these are referred to as the full equations of motion since they characterize the full attitude of the rigid pendulum. As there is a rotational symmetry corresponding to the group of rotations about the vertical axis through the pivot and the associated angular momentum component is conserved, it is possible to obtain a lower dimensional reduced model for the rigid pendulum. This Lagrange–Poincaré reduction is based on the fact that the dynamics and kinematics equations can be written in terms of the reduced attitude vector $\Gamma = R^T e_3 \in S^2$, which is the unit vector that expresses the gravity direction in the body-fixed frame [14].

Specifically, denote the group action of $\theta \in S^1$ on $SO(3)$ by $\Phi_\theta : SO(3) \rightarrow SO(3)$, $\Phi_\theta(R) = \exp(\theta \hat{e}_3)R$. This induces an equivalence class by identifying elements of $SO(3)$ that belong to the same orbit; explicitly, for $R_1, R_2 \in SO(3)$, we write $R_1 \sim R_2$ if there exists a $\theta \in S^1$ such that $\Phi_\theta(R_1) = R_2$. The *orbit space* $SO(3)/S^1$ is the set of equivalence classes,

$$[R] \triangleq \{\Phi_\theta(R) \in SO(3) : \theta \in S^1\}. \quad (4.1)$$

For this equivalence relation, it is easy to see that $R_1 \sim R_2$ if and only if $R_1^T e_3 = R_2^T e_3$ and hence the equivalence class in (4.1) can alternately, be expressed as

$$[R] \triangleq \{R_s \in SO(3) : R_s^T e_3 = R^T e_3\}. \quad (4.2)$$

Thus, for each $R \in SO(3)$, $[R]$ can be identified with $\Gamma = R^T e_3 \in S^2$ and hence $SO(3)/S^1 \cong S^2$. This group action induces a projection $\Pi : SO(3) \rightarrow SO(3)/S^1 \cong S^2$ given by $\Pi(R) = R^T e_3$.

Proposition 4 ([7]). *The dynamics of the 3D pendulum given by (3.1) and (3.2) induce a flow on the quotient space $TSO(3)/S^1$, through the projection $\pi : TSO(3) \rightarrow TSO(3)/S^1$ defined as $\pi(R, \Omega) = (R^T e_3, \Omega)$, given by the dynamics*

$$J\dot{\omega} = J\omega \times \omega + mg\rho \times \Gamma, \quad (4.3)$$

and the kinematics for the reduced attitude

$$\dot{\Gamma} = \Gamma \times \omega. \quad (4.4)$$

Furthermore, $TSO(3)/S^1 \cong S^2 \times \mathbb{R}^3$.

Equations (4.3) and (4.4) are expressed in a non-canonical form; they are referred to as the reduced attitude dynamics of the 3D pendulum on $TSO(3)/S^1$.

4.1. Special Cases of the 3D Pendulum. Three interesting special cases are now examined. Suppose that the 3D pendulum is axisymmetric, that is two of the principal moments of inertia of the pendulum are identical and the pivot is located on the axis of symmetry of the pendulum. Assume that the body-fixed axes are selected so that $J = \text{diag}(J_t, J_t, J_a)$ and $\rho = \rho_s e_3$ where ρ_s is a positive scalar constant. Consequently, equation (4.3) can be written in scalar form, as

$$\begin{cases} J_t \dot{\omega}_x = (J_t - J_a) \omega_y \omega_z - mg\rho_s \Gamma_y, \\ J_t \dot{\omega}_y = (J_a - J_t) \omega_z \omega_x + mg\rho_s \Gamma_x, \\ J_a \dot{\omega}_z = 0. \end{cases} \quad (4.5)$$

From the last equation in (4.5), we see that the component of the 3D pendulum angular velocity vector about its axis of symmetry is constant. This means that a constant ω_z defines an invariant manifold for the 3D pendulum dynamics. The special case that $\omega_z = c$, where $c \in \mathbb{R}$, leads to invariant dynamics of the axisymmetric 3D pendulum, described as follows:

Proposition 5. *Assume the 3D pendulum has a single axis of symmetry and the pivot and the center of mass are located on the axis of symmetry of the pendulum as above. The equations of motion of the 3D pendulum define an induced flow on the fiber bundle $S^2 \times \mathbb{R}^2$ corresponding to $\omega_z = c$, where $c \neq 0$, given by the equations*

$$\begin{aligned} J_t \dot{\omega}_x &= c(J_t - J_a) \omega_y - mg\rho_s \Gamma_y, \\ J_t \dot{\omega}_y &= c(J_a - J_t) \omega_x + mg\rho_s \Gamma_x, \\ \dot{\Gamma} &= \Gamma \times [\omega_x \quad \omega_y \quad c]^T. \end{aligned}$$

These equations describe the dynamics of a *spinning top* where $c \in \mathbb{R}$ denotes the spin rate.

If the spin rate of the 3D pendulum about its axis of symmetry is zero, the following result is obtained.

Proposition 6. *Assume the 3D pendulum has a single axis of symmetry and the pivot and the center of mass are located on the axis of symmetry of the pendulum as above. The equations of motion of the 3D pendulum define an induced flow on the fiber bundle $S^2 \times \mathbb{R}^2$ corresponding to $\omega_z = 0$, given by the equations*

$$\begin{aligned} J_t \dot{\omega}_x &= -mg\rho_s \Gamma_y, \\ J_t \dot{\omega}_y &= mg\rho_s \Gamma_x, \\ \dot{\Gamma} &= \Gamma \times [\omega_x \quad \omega_y \quad 0]^T. \end{aligned}$$

These equations describe the dynamics of a 2D *spherical pendulum*.

Now assume the spin rate of the 3D pendulum about its axis of symmetry is zero and, in addition, $\omega_x(0) = 0$ and $\Gamma_y(0) = 0$ for the axisymmetric 3D pendulum. Then Proposition 6 yields invariant dynamics of the axisymmetric 3D pendulum such that $\omega_x(t) = \Gamma_y(t) = 0$ for all $t \geq 0$. Therefore Γ can be parameterized by an angle θ as $\Gamma = [-\sin \theta \quad 0 \quad \cos \theta]^T$. This yields the following result.

Proposition 7. *Assume the 3D pendulum has a single axis of symmetry and the pivot is located on the axis of symmetry of the pendulum as above. The equations of motion of the rigid pendulum define an induced flow on the tangent bundle TS^1 corresponding to $\omega_x = 0$, $\omega_z = 0$ given by the equations*

$$\begin{aligned} J_t \dot{\omega}_y &= -mg\rho_s \sin \theta, \\ \dot{\theta} &= \omega_y. \end{aligned}$$

These equations describe the dynamics of a 1D *planar pendulum*.

Thus for an axially symmetric 3D pendulum with the pivot located on the axis of symmetry, the well known 2D spherical pendulum and the 1D planar pendulum can be viewed as special cases of the 3D pendulum dynamics. For an axially symmetric 3D pendulum with the pivot located on the axis of symmetry, the induced dynamics corresponding to a nonzero constant value of ω_z is fundamentally different from the dynamics of the spherical pendulum; these dynamics seem not to have been previously studied. It should be emphasized that if the 3D pendulum is asymmetric then the dynamics are general in the sense that neither the 2D spherical pendulum dynamics nor the 1D planar pendulum dynamics are special cases.

4.2. Invariants of the Lagrange–Poincaré Reduced Model. In a previous section, we obtained two integrals of motion for the full model of the 3D pendulum. In this section we summarize similar results for the Lagrange–Poincaré reduced model of the 3D pendulum considered here.

Proposition 8. *The total energy*

$$E = \frac{1}{2} \omega^\top J \omega - mg \rho^\top \Gamma, \quad (4.6)$$

and the component of the angular momentum vector about the vertical axis through the pivot

$$h = \omega^\top J \Gamma.$$

are each constant along trajectories of the Lagrange–Poincaré reduced model of the 3D pendulum given by (4.3) and (4.4).

4.3. Equilibria of the Lagrange–Poincaré Reduced Model. We study the equilibria of the Lagrange–Poincaré reduced equations of motion of the 3D pendulum given by (4.3) and (4.4). Equating the RHS of (4.3) and (4.4) to zero yields that a natural equilibrium (Γ_e, ω_e) satisfies

$$J \omega_e \times \omega_e + mg \rho \times \Gamma_e = 0, \quad (4.7)$$

$$\Gamma_e \times \omega_e = 0. \quad (4.8)$$

Equation (4.8) implies that $\omega_e = k \Gamma_e$, where $k \in \mathbb{R}$, and substituting this into (4.7) yields

$$k^2 J \Gamma_e \times \Gamma_e + mg \rho \times \Gamma_e = 0. \quad (4.9)$$

Note that depending on whether k is equal to zero or not, one can obtain *static* ($\omega_e \equiv 0$) or *dynamic* ($\omega_e \neq 0$) equilibrium. The dynamic case corresponds to relative equilibria [11] of the 3D pendulum.

Without loss of generality, we assume that the moment of inertia matrix is diagonal, i.e. $J = \text{diag}(J_1, J_2, J_3)$, where $J_1 \geq J_2 \geq J_3 > 0$. This is achieved by choosing the body-fixed reference frame such that the body-fixed axes lie along the principal axes. Note that the vector from the pivot point to the center of mass ρ may not lie along any principal axis. The following result describes the equilibria structure of the Lagrange–Poincaré reduced equations.

Proposition 9. *Consider the Lagrange–Poincaré model of the 3D pendulum given by (4.3) and (4.4). The equilibria (Γ_e, ω_e) of the Lagrange–Poincaré model are given as follows.*

1. *The hanging equilibrium:* $\left(\frac{\rho}{\|\rho\|}, 0\right)$,
2. *The inverted equilibrium:* $\left(-\frac{\rho}{\|\rho\|}, 0\right)$,
3. *Two relative equilibria:*

$$\left\{ \left(-\frac{J^{-1}\rho}{\|J^{-1}\rho\|}, \sqrt{\frac{mg}{\|J^{-1}\rho\|}} J^{-1}\rho \right), \left(-\frac{J^{-1}\rho}{\|J^{-1}\rho\|}, -\sqrt{\frac{mg}{\|J^{-1}\rho\|}} J^{-1}\rho \right) \right\}, \quad (4.10)$$

4. *One dimensional relative equilibrium manifolds:*

$$\left(-\text{sgn}(\alpha) \frac{n_\alpha}{\|n_\alpha\|}, \sqrt{\frac{mg}{\|n_\alpha\|}} n_\alpha \right), \quad (4.11)$$

where $n_\alpha = (J - \frac{1}{\alpha} I_{3 \times 3})^{-1} \rho \in \mathbb{R}^3$ corresponding to $\alpha \in \mathcal{L}_i$, $i \in \{1, 2, 3, 4\}$ and

$$\mathcal{L}_1 = (-\infty, 0) \cup (\frac{1}{J_3}, \infty), \quad \mathcal{L}_2 = (0, \frac{1}{J_1}), \quad \mathcal{L}_3 = (\frac{1}{J_1}, \frac{1}{J_2}), \quad \mathcal{L}_4 = (\frac{1}{J_2}, \frac{1}{J_3}).$$

Also, $\text{sgn}(\cdot)$ denotes the sign function.

5. *One dimensional relative equilibrium manifolds:*

$$\left(-\text{sgn}(\alpha) \frac{n_\alpha}{\|n_\alpha\|}, -\sqrt{\frac{mg}{\|n_\alpha\|}} n_\alpha \right), \quad (4.12)$$

where n_α and α are as given above in Case 4.

The families of equilibria given in (4.11) and (4.12) converge to the hanging equilibrium and the inverted equilibrium when $\alpha \rightarrow 0$, and they converge to the third equilibria given in (4.10), when $\alpha \rightarrow \pm\infty$. If the vector from the pivot to the center of mass ρ , lies on a principal axis, i.e. $\rho \times e_i = 0$ for some $i \in \{1, 2, 3\}$, then (4.11) and (4.12) can be rewritten as $\{(e_i, \gamma e_i), (-e_i, \gamma e_i)\}$ for $\gamma \in \mathbb{R}$.

Furthermore, there exist additional equilibria under the following assumptions on the moment of inertia matrix J and the vector from the pivot to the center of mass $\rho = [\rho_1 \ \rho_2 \ \rho_3]^T$.

6. J_1, J_2 and J_3 are distinct and $\rho_i = 0$. Then there exist one-dimensional relative equilibrium manifolds:

$$\left\{ \left(-\frac{p_i}{\|p_i\|}, \sqrt{\frac{mg}{\|p_i\|}} p_i \right), \left(-\frac{p_i}{\|p_i\|}, -\sqrt{\frac{mg}{\|p_i\|}} p_i \right) \right\} \quad (4.13)$$

for $i \in \{1, 2, 3\}$, where $p_1 = (\gamma, \frac{\rho_2}{J_2 - J_1}, \frac{\rho_3}{J_3 - J_1})$, $p_2 = (\frac{\rho_1}{J_1 - J_2}, \gamma, \frac{\rho_3}{J_3 - J_2})$, $p_3 = (\frac{\rho_1}{J_1 - J_3}, \frac{\rho_2}{J_2 - J_3}, \gamma)$ and $\gamma \in \mathbb{R}$.

7. $J_1 = J_2 \neq J_3$.

- (a) If $\rho_1 = \rho_2 = 0$. Then there exist two-dimensional relative equilibrium manifolds:

$$\left\{ \left(-\frac{q}{\|q\|}, \sqrt{\frac{mg}{\|q\|}} q \right), \left(-\frac{q}{\|q\|}, -\sqrt{\frac{mg}{\|q\|}} q \right) \right\}$$

where $q = (\gamma, \delta, \frac{\rho_3}{J_3 - J_1})$ and $\gamma, \delta \in \mathbb{R}$.

- (b) If $\rho_3 = 0$. Then there exist one-dimensional relative equilibrium manifolds:

$$\left\{ \left(-\frac{r}{\|r\|}, \sqrt{\frac{mg}{\|r\|}} r \right), \left(-\frac{r}{\|r\|}, -\sqrt{\frac{mg}{\|r\|}} r \right) \right\}$$

where $r = (\frac{\rho_1}{J_1 - J_3}, \frac{\rho_2}{J_1 - J_3}, \gamma)$ and $\gamma \in \mathbb{R}$.

Proof. From (4.9), an equilibrium (Γ_e, ω_e) satisfies

$$k^2 J \Gamma_e + mg \rho = k_1 \Gamma_e, \quad (4.14)$$

for a constant $k_1 \in \mathbb{R}$. We solve this equation to obtain the expression for an equilibrium attitude Γ_e for two cases; when $k_1 = 0$ and when $k_1 \neq 0$. The corresponding value of the constant k yields the expression for the equilibrium angular velocity as $\omega_e = k \Gamma_e$.

Equilibria 3: Suppose $k_1 = 0$. It follows that $k \neq 0$ from (4.14). Thus, we have $\Gamma_e = -\frac{mg}{k^2} J^{-1} \rho$. Since $\|\Gamma_e\| = 1$, we obtain $k^2 = mg \|J^{-1} \rho\|$, which gives (4.10).

Equilibria 1, 2, 4 and 5: Suppose $k_1 \neq 0$. If $k = 0$, (4.14) yields the hanging and the inverted equilibrium. Suppose $k \neq 0$. Define $\alpha = \frac{k^2}{k_1} \in \mathbb{R} \setminus \{0\}$, and $v = k_1 \Gamma_e \in \mathbb{R}^3$. Then, (4.14) can be written as

$$(\alpha J - I_{3 \times 3}) v = -mg \rho. \quad (4.15)$$

Note that for $\alpha \in \mathbb{R} \setminus \{0, \frac{1}{J_1}, \frac{1}{J_2}, \frac{1}{J_3}\}$ the matrix $(J - \frac{1}{\alpha} I_{3 \times 3})$ is invertible. Then, (4.15) can be solved to obtain $v = -\frac{mg}{\alpha} (J - \frac{1}{\alpha} I_{3 \times 3})^{-1} \rho$. Since $\|\Gamma_e\| = 1$, we have $\|v\| = \|k_1 \Gamma_e\| = |k_1|$. We consider two sub-cases; when $k_1 > 0$, and $k_1 < 0$.

If $k_1 > 0$, we have $k_1 = \|v\|$ and $\alpha > 0$. Thus, we obtain the expression for equilibria attitudes as

$$\Gamma_e = \frac{v}{\|v\|} = -\frac{n_\alpha}{\|n_\alpha\|} = -\text{sgn}(\alpha) \frac{n_\alpha}{\|n_\alpha\|}. \quad (4.16)$$

where $n_\alpha = (J - \frac{1}{\alpha} I_{3 \times 3})^{-1} \rho \in \mathbb{R}^3$. Since $k^2 = \alpha k_1 = \alpha \|v\|$, we obtain the expression for equilibria angular velocities as

$$\omega_e = k \Gamma_e = \mp \sqrt{\alpha \|v\|} \frac{n_\alpha}{\|n_\alpha\|} = \mp \sqrt{\frac{mg}{\|n_\alpha\|}} n_\alpha. \quad (4.17)$$

Thus, (4.16) and (4.17) correspond to the families of equilibria given by (4.11) and (4.12) for $\alpha > 0$. Consider the limiting case when $\alpha \rightarrow \infty$. We have

$$\lim_{\alpha \rightarrow \infty} -\frac{n_\alpha}{\|n_\alpha\|} = \lim_{\alpha \rightarrow \infty} -\frac{(J - I_{3 \times 3}/\alpha)^{-1}\rho}{\|(J - I_{3 \times 3}/\alpha)^{-1}\rho\|} = -\frac{J^{-1}\rho}{\|J^{-1}\rho\|}.$$

Similarly,

$$\lim_{\alpha \rightarrow \infty} \sqrt{\frac{mg}{\|n_\alpha\|}} n_\alpha = \sqrt{\frac{mg}{\|J^{-1}\rho\|}} J^{-1}\rho.$$

Thus, as $\alpha \rightarrow \infty$, (4.16) and (4.17) converges to the first relative equilibria given in (4.10).

Similarly, if $k_1 < 0$, we have $k_1 = -\|v\|$, $\alpha < 0$, and $k^2 = -\alpha\|v\|$. Thus, the relative equilibria are described by

$$\Gamma_e = -\frac{v}{\|v\|} = \frac{n_\alpha}{\|n_\alpha\|} = -\text{sgn}(\alpha) \frac{n_\alpha}{\|n_\alpha\|}, \quad \omega_e = \pm \sqrt{\frac{mg}{\|n_\alpha\|}} n_\alpha, \quad (4.18)$$

which corresponds to the families of equilibria given by (4.11) and (4.12) for $\alpha < 0$. It can be similarly shown that they converges to the third relative equilibria given by (4.10) as $\alpha \rightarrow -\infty$.

Next, consider (4.11) and (4.12) as $\alpha \rightarrow 0$. Expressing $n_\alpha = \alpha(\alpha J - I_{3 \times 3})^{-1}\rho$, we obtain

$$\lim_{\alpha \rightarrow 0^+} -\text{sgn}(\alpha) \frac{n_\alpha}{\|n_\alpha\|} = \lim_{\alpha \rightarrow 0^+} -\frac{(\alpha J - I_{3 \times 3})^{-1}\rho}{\|(\alpha J - I_{3 \times 3})^{-1}\rho\|} = -\frac{\rho}{\|\rho\|},$$

which corresponds to the inverted attitude. Similarly,

$$\lim_{\alpha \rightarrow 0^-} -\text{sgn}(\alpha) \frac{n_\alpha}{\|n_\alpha\|} = \lim_{\alpha \rightarrow 0^-} \frac{(\alpha J - I_{3 \times 3})^{-1}\rho}{\|(\alpha J - I_{3 \times 3})^{-1}\rho\|} = \frac{\rho}{\|\rho\|},$$

which corresponds to the hanging attitude. For the angular velocity term,

$$\lim_{\alpha \rightarrow 0} \sqrt{\frac{mg}{\|n\|}} n = \lim_{\alpha \rightarrow 0} \sqrt{mg\|n\|} \frac{n}{\|n\|} = \pm \frac{\rho}{\|\rho\|} \lim_{\alpha \rightarrow 0} \sqrt{mg\|\alpha\rho\|} = 0.$$

Thus, as $\alpha \rightarrow 0^-$, (4.11) and (4.12) yields the hanging equilibrium given in case (1), and similarly, as $\alpha \rightarrow 0^+$, (4.11) and (4.12) yields the inverted equilibrium given in case (2).

Now suppose the vector from the pivot to the center of mass ρ , lies on a principal axis, i.e. $\rho \times e_i = 0$ for some $i \in \{1, 2, 3\}$. Then the vector ρ can be expressed as $\rho = s e_i$, where $s \in \mathbb{R}$. Then for all $\alpha \in \mathbb{R} \setminus \{0, \frac{1}{J_1}, \frac{1}{J_2}, \frac{1}{J_3}\}$, $(\alpha J - I_{3 \times 3})$ is an invertible diagonal matrix, and hence $n_\alpha = \frac{1}{\alpha}(\alpha J - I_{3 \times 3})^{-1}\rho = \frac{s}{\alpha(\alpha J_i - 1)} e_i$. Then, it follows from (4.11) and (4.12) that the equilibria can be rewritten as $\{(e_i, \gamma e_i), (-e_i, \gamma e_i)\}$ for $\gamma \in \mathbb{R}$.

The solution of (4.15) for $\alpha \in \mathbb{R}$ yields all possible equilibria of (4.3) and (4.4). Equation (4.11) and (4.12) present the solution of (4.15) for all $\alpha \in \mathbb{R} \setminus \{0, \frac{1}{J_1}, \frac{1}{J_2}, \frac{1}{J_3}\}$. As shown before, $\alpha = 0$ yields the hanging and the inverted equilibrium. If $\alpha \in \{\frac{1}{J_1}, \frac{1}{J_2}, \frac{1}{J_3}\}$, (4.15) can have solutions under certain conditions. This yields the additional equilibria of (4.3) and (4.4) given in Case 6 and 7.

Equilibria 6: Suppose J_1, J_2 and J_3 are distinct. Then it is easy to see that for $\alpha = 1/J_1$, (4.15) has a solution iff $\rho_1 = 0$. In this case, (4.15) can be written as

$$\begin{bmatrix} 0 & 0 & 0 \\ 0 & J_2 - J_1 & 0 \\ 0 & 0 & J_3 - J_1 \end{bmatrix} v = -mgJ_1 \begin{bmatrix} 0 \\ \rho_2 \\ \rho_3 \end{bmatrix}.$$

Since $\alpha > 0$, it can be shown as in (4.16) that $\Gamma_e = -\frac{p_1}{\|p_1\|}$ and $\omega_e = \pm \sqrt{\frac{mg}{\|p_1\|}} p_1$, where $p_1 = (\gamma, \frac{\rho_2}{J_2 - J_1}, \frac{\rho_3}{J_3 - J_1})$ and $\gamma \in \mathbb{R}$. Similarly, one can yield solutions of (4.15) for the case where $\alpha = 1/J_2$ and $\alpha = 1/J_3$ iff $\rho_2 = 0$

and $\rho_3 = 0$, respectively. Thus for distinct principal moments of inertia, one obtains the equilibria given in case 5, corresponding to the condition $\rho_i = 0$ where $i \in \{1, 2, 3\}$.

Equilibria 7: (a) Suppose $J_1 = J_2 \neq J_3$. Then it is easy to see that for $\alpha = 1/J_1 = 1/J_2$, (4.15) has a solution iff $\rho_1 = \rho_2 = 0$. In this case, (4.15) can be written as

$$\begin{bmatrix} 0 & 0 & 0 \\ 0 & 0 & 0 \\ 0 & 0 & J_3 - J_1 \end{bmatrix} v = -mgJ_1 \begin{bmatrix} 0 \\ 0 \\ \rho_3 \end{bmatrix}.$$

Since $\alpha > 0$, it can be shown as in (4.16) that $\Gamma_e = -\frac{q}{\|q\|}$ and $\omega_e = \pm \sqrt{\frac{mg}{\|q\|}}q$, where $q = (\gamma, \delta, \frac{\rho_3}{J_3 - J_1})$ and $\gamma, \delta \in \mathbb{R}$.

(b) Similar to above, one can yield solutions of (4.15) for the case where $\alpha = 1/J_3$ iff $\rho_3 = 0$.

Thus for $J_1 = J_2 \neq J_3$, one obtains the equilibria given in case 7(a) and 7(b) under the specified conditions. Finally for the case where $J_1 = J_2 = J_3$, there are no additional solutions of (4.15) for $\alpha \in \{\frac{1}{J_1}, \frac{1}{J_2}, \frac{1}{J_3}\}$. \square

Numerical example. We show the equilibrium structure of a particular 3D pendulum model. We choose an elliptic cylinder with its semimajor axis $a = 0.8m$, semi-minor axis $b = 0.2m$, and height $0.6m$. The pivot point is located at the surface of the upper ellipse, and it is offset from the center by $[-\frac{a}{2}, \frac{b}{2}, 0]$. The moment of inertia is given by $J = \text{diag}(0.4486, 0.3943, 0.0772)$ and the vector from the pivot to the mass center is $\rho = [-0.0140, 0.1044, 0.4989]$. One of hanging attitudes is shown in Fig. 4.1(a).

Figures 4.1(b)–4.1(d) show the relative equilibria attitudes on S^2 , where the top corresponds $\Gamma = -e_3$, and the bottom corresponds to $\Gamma = e_3$. The inverted equilibrium is denoted by a red dot, and the hanging equilibrium is denoted by a blue dot, and the equilibria of (4.10) are located at the intersection of the blue line and the red line in Fig. 4.1(c). The families of the relative equilibria given by (4.11) and (4.12) are shown by the four segments of solid lines corresponding to \mathcal{L}_i , where $i \in \{1, 2, 3, 4\}$ and the value of α is represented by color-shading; α varies from $-\infty$ (blue color) to ∞ (red color). Note that the reduced attitude in both (4.11) and (4.12), are the same and these families of equilibria only differ by a sign in the angular velocity vector at the equilibrium.

The relative equilibria for $\alpha \in (-\infty, 0)$ are shown by a segment of a blue line in Fig. 4.1(c), which starts from the third equilibria given by (4.10), and converges to the inverted equilibrium. For $\alpha \in (0, \frac{1}{J_3})$, three disjoint segments of the relative equilibria attitudes are shown in Fig. 4.1(d); $\alpha \in (0, \frac{1}{J_1}) = \mathcal{L}_2$ (upper-left, moving counter-clockwise from blue to cyan), $\alpha \in (\frac{1}{J_1}, \frac{1}{J_2}) = \mathcal{L}_3$ (upper-right, moving counter-clockwise from cyan to green), and $\alpha \in (\frac{1}{J_2}, \frac{1}{J_3}) = \mathcal{L}_4$ (lower center, moving upward from green to orange). The relative equilibria attitudes for $\alpha \in (\frac{1}{J_3}, \infty)$ are shown in Fig. 4.1(c) by a red line segment, which converges to the blue line at the third equilibrium given by (4.10).

Since no component of the center of mass vector vanishes, there are no additional equilibria. In summary, the hanging attitude, the inverted attitude, and the attitude given by (4.10) are equilibrium attitudes, and there are four mutually disjoint equilibrium attitude segments corresponding to \mathcal{L}_i , where $i \in \{1, 2, 3, 4\}$.

Relation to the equilibrium manifolds of the full model. Let

$$\Gamma_h \triangleq \frac{\rho}{\|\rho\|}, \text{ and } \Gamma_i \triangleq -\frac{\rho}{\|\rho\|}.$$

Then it follows from Proposition 9 that $(\Gamma_h, 0)$ and $(\Gamma_i, 0)$ are equilibria of the Lagrange–Poincaré reduced model of the 3D pendulum. These are called the hanging equilibrium and the inverted equilibrium of the Lagrange–Poincaré reduced model, respectively.

Let $(R_e, 0)$ denote an equilibrium in either the hanging equilibrium manifold or the inverted equilibrium manifold of the full equations (3.1) and (3.2) and $\pi : TSO(3) \rightarrow TSO(3)/S^1$ be the projection as in Proposition 4. Then, it can be shown that either $\pi(R_e, 0) = (\Gamma_h, 0)$ or $\pi(R_e, 0) = (\Gamma_i, 0)$. Thus, the hanging and the inverted equilibrium manifold of the full equations are identified with the hanging and the inverted equilibrium of the Lagrange–Poincaré reduced equations.

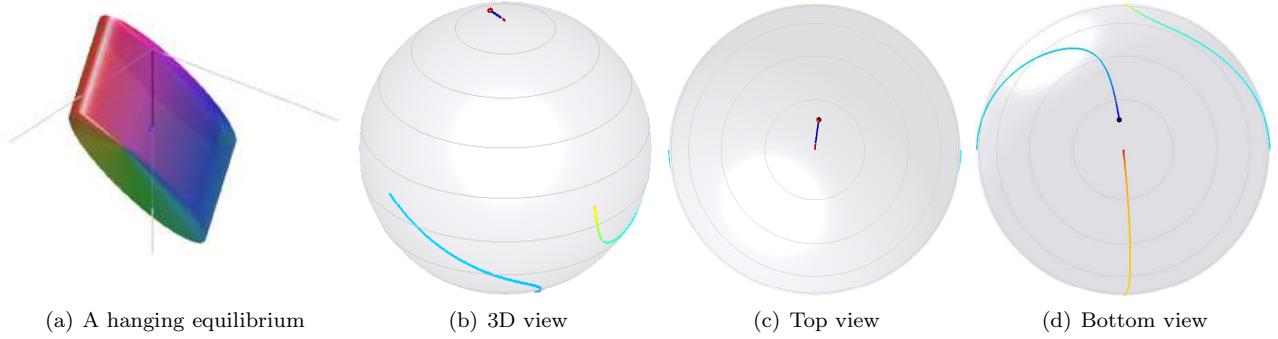


FIG. 4.1. *Relative equilibria attitudes for an elliptic cylinder 3D pendulum model*

To study the properties of the equilibrium manifolds, it is advantageous to consider the hanging and the inverted equilibrium of the equations of the 3D pendulum in terms of the reduced attitude as in (4.3) and (4.4). The following result provides the identification.

Proposition 10 ([7]). *The hanging equilibrium manifold and the inverted equilibrium manifold of the 3D pendulum given by (3.1) and (3.2) are identified with the hanging equilibrium $(\Gamma_h, 0)$ and the inverted equilibrium $(\Gamma_i, 0)$ of the reduced attitude equations given by (4.3) and (4.4).*

4.4. Local Analysis of the Lagrange–Poincaré Reduced Model near an Equilibrium. In the last section, we showed that the Lagrange–Poincaré reduced model of the 3D pendulum can have equilibria with non-zero angular velocities. Also, there are only two *static* equilibria, namely the hanging equilibrium and the inverted equilibrium. As stated in Proposition 10, these equilibria correspond to the disjoint equilibrium manifolds of the full equations of the 3D pendulum.

We next focus on these static equilibria of the Lagrange–Poincaré reduced equations. The identification mentioned in Proposition 10 relates properties of the equilibrium manifolds of the full equations and the equilibria of the Lagrange–Poincaré reduced equations. We deduce the stability of the hanging and the inverted equilibrium manifolds of the full equations by studying the stability property of the hanging equilibrium and the inverted equilibrium of the Lagrange–Poincaré reduced equations.

Consider the linearization of (4.3)–(4.4) about an equilibrium $(\Gamma_h, 0) = (R_e^T e_3, 0)$, where $(R_e, 0)$ is an equilibrium of the hanging equilibrium manifold H . Since $\dim[TSO(3)/S^1] = 5$, the linearization of (4.3)–(4.4) about $(\Gamma_h, 0)$ evolves on \mathbb{R}^5 .

Proposition 11. *The linearization of the Lagrange–Poincaré reduced equations for the 3D pendulum, about the equilibrium $(\Gamma_h, 0) = (R_e^T e_3, 0)$ described by equations (4.3)–(4.4) can be expressed using $(x_1, x_2, \dot{x}_1, \dot{x}_2, \dot{x}_3) \in \mathbb{R}^5$ according to (3.22)–(3.24).*

Proof. Consider a perturbation in terms of the perturbation parameter $\varepsilon \in \mathbb{R}$ as before. Let $(R^\varepsilon(t), \omega^\varepsilon(t))$ denote the perturbed solution of (3.1)–(3.2). Since $\Gamma = R^T e_3$, the perturbed solution of (4.3)–(4.4) is given by $(\Gamma^\varepsilon(t), \omega^\varepsilon(t))$ where $\Gamma^\varepsilon(t) = (R^\varepsilon)^T(t) e_3$. Define the perturbation variables $\Delta\omega(t) \triangleq \omega_\varepsilon^0(t)$ and $\Delta\Gamma(t) \triangleq \Gamma_\varepsilon^0(t) = (R_\varepsilon^0)^T(t) e_3$. From definition of $\Delta\Theta$ in Subsection 3.3, note that

$$\Delta\Gamma = -\widehat{\Delta\Theta} R_e^T e_3 = \widehat{\Gamma}_h \Delta\Theta \in T_{\Gamma_h} S^2.$$

Then from (3.19) and the definition of $\Delta\Gamma$, it can be easily shown that the linearization of (4.3)–(4.4) is given by

$$J\Delta\dot{\omega} = mg\widehat{\rho} \Delta\Gamma, \quad (4.19)$$

$$\Delta\dot{\Gamma} = \widehat{\Gamma}_h \Delta\omega. \quad (4.20)$$

Next, we express (4.19) and (4.20) in terms of (x, \dot{x}) . Specifically, we show that $(\Delta\Gamma, \Delta\omega) \in T_{\Gamma_h} S^2 \times \mathbb{R}^3$ can be expressed using $(x_1, x_2, \dot{x}_1, \dot{x}_2, \dot{x}_3) \in \mathbb{R}^5$.

Since $x = M^T \Delta \Theta$, and M is nonsingular, $\Delta \omega = M^{-T} \dot{x}$ and $\Delta \Gamma = \widehat{\Gamma}_h M^{-T} x$. We now give an orthogonal decomposition of the vector $\Delta \Theta = M^{-T} x$ into a component along the vector ρ and a component normal to the vector ρ . This decomposition is

$$M^{-T} x = -\frac{\widehat{\rho}^2}{\|\rho\|^2} (M^{-T} x) + \frac{1}{\|\rho\|^2} [\rho^T (M^{-T} x)] \rho,$$

where $\frac{1}{\|\rho\|^2} [\rho^T (M^{-T} x)] \rho \in \text{span}\{\rho\}$ and $-\frac{\widehat{\rho}^2}{\|\rho\|^2} (M^{-T} x) \in \text{span}\{\rho\}^\perp$. Thus,

$$\Delta \Gamma = \widehat{\Gamma}_h \Delta \Theta = \frac{\widehat{\rho}}{\|\rho\|} M^{-T} x = \frac{1}{mg \|\rho\|^2} \widehat{\rho} M \Lambda x,$$

does not depend on x_3 since $\Lambda = \text{diag}(mgl_1, mgl_2, 0)$. Thus, we can express the linearization of (4.3)–(4.4) at $(\Gamma_h, 0) = (R_e^T e_3, 0)$ in terms of the variables $(x_1, x_2, \dot{x}_1, \dot{x}_2, \dot{x}_3)$ according to (3.22)–(3.24). \square

Remark 1. Note that due to our careful choice of variables, one can discard x_3 from (3.22)–(3.24) when studying the stability properties of the inverted equilibrium manifold. Thus, x_3 corresponds to a component of the perturbation in the attitude that is tangential to the inverted equilibrium manifold. However, the angular velocity corresponding to x_3 given by \dot{x}_3 is retained.

Summarizing the above, the linearization of (4.3)–(4.4) about the hanging equilibrium $(\Gamma_h, 0)$ is expressed as

$$\ddot{x}_1 + mgl_1 x_1 = 0, \tag{4.21}$$

$$\ddot{x}_2 + mgl_2 x_2 = 0, \tag{4.22}$$

$$\dot{x}_3 = 0. \tag{4.23}$$

It is clear that due to the presence of zero and imaginary eigenvalues, one cannot arrive at a conclusion about the stability of the hanging equilibrium $(\Gamma_h, 0)$ from the linear analysis. Therefore we next consider Lyapunov analysis.

Proposition 12. *The hanging equilibrium $(\Gamma_h, 0) = \left(\frac{\rho}{\|\rho\|}, 0\right)$, of the reduced dynamics of the 3D pendulum described by equations (4.3) and (4.4) is stable in the sense of Lyapunov.*

Proof. Consider the candidate Lyapunov function

$$V(\Gamma, \omega) = \frac{1}{2} \omega^T J \omega + mg(\|\rho\| - \rho^T \Gamma). \tag{4.24}$$

Note that $V(\Gamma_h, 0) = 0$ and $V(\Gamma, \omega) > 0$ elsewhere. Furthermore, the derivative along a solution of (4.3) and (4.4) is given by

$$\begin{aligned} \dot{V}(\Gamma, \omega) &= \omega^T J \dot{\omega} - mg \rho^T \dot{\Gamma}, \\ &= \omega^T (J \omega \times \omega + mg \rho \times \Gamma) - mg \rho^T (\Gamma \times \omega), \\ &= \omega^T mg \rho \times \Gamma - mg \rho^T \Gamma \times \omega = 0. \end{aligned}$$

Thus, the hanging equilibrium is Lyapunov stable. \square

Remark 2. Note that combining Proposition 12 with Proposition 10 immediately confirms the stability result for the hanging equilibrium manifold in Proposition 2.

We next study the local properties of the Lagrange–Poincaré reduced equations of the 3D pendulum near the inverted equilibrium $(\Gamma_i, 0)$. Consider the linearization of (4.3)–(4.4) about an equilibrium $(\Gamma_i, 0) = (R_e^T e_3, 0)$, where $(R_e, 0)$ is an equilibrium of the inverted equilibrium manifold I. A result similar to Proposition 11 follows.

Proposition 13. *The linearization of the Lagrange–Poincaré reduced equations for the 3D pendulum, about the equilibrium $(\Gamma_i, 0) = (R_e^T e_3, 0)$ described by equations (4.3)–(4.4) can be expressed using $(x_1, x_2, \dot{x}_1, \dot{x}_2, \dot{x}_3) \in \mathbb{R}^5$ according to (3.26)–(3.28).*

Summarizing the above, the linearization of (4.3)–(4.4) about the inverted equilibrium $(\Gamma_i, 0)$ is expressed as

$$\ddot{x}_1 - mgl_1x_1 = 0, \quad (4.25)$$

$$\ddot{x}_2 - mgl_2x_2 = 0, \quad (4.26)$$

$$\dot{x}_3 = 0. \quad (4.27)$$

Note that the inverted equilibrium of the Lagrange–Poincaré reduced equations has two negative eigenvalues, two positive eigenvalues and a zero eigenvalue. Thus, the inverted equilibrium $(\Gamma_i, 0)$ is unstable and locally there exists a two dimensional stable manifold, a two dimensional unstable manifold and a one dimensional center manifold.

Proposition 14. *The inverted equilibrium $(\Gamma_i, 0) = \left(-\frac{\rho}{\|\rho\|}, 0\right)$, of the Lagrange–Poincaré reduced dynamics of the 3D pendulum described by equations (4.3) and (4.4) is unstable.*

Remark 3. Note that combining Proposition 14 with Proposition 10 immediately confirms the result that the inverted equilibrium manifold I of the full equations for the 3D pendulum given by (3.1)–(3.2) is unstable.

We have analyzed the local stability properties of the hanging equilibrium and of the inverted equilibrium. We have not analyzed local stability properties of any other equilibrium solutions, but this analysis can easily be carried out using the methods that have been introduced.

5. Lagrange–Routh Reduced 3D Pendulum Dynamics on TS^2 . In the previous sections we studied the full and the Lagrange–Poincaré reduced equations of motion of the 3D pendulum. These involved the study of the dynamics of the 3D pendulum on $TSO(3)$ and on $TSO(3)/S^1$, respectively, using (R, ω) and $(\Gamma, \dot{\Gamma})$ to express the equations of motion. In this section, we present Lagrange–Routh reduction of the 3D pendulum, and we study the equations of motion that describe the evolution of $(\Gamma, \dot{\Gamma}) \in TS^2$.

5.1. Lagrange–Routh Reduction of the 3D pendulum. The key feature of Lagrange–Routh reduction is reducing the configuration space into the quotient space induced by the symmetry action. The resulting equations of motion on the reduced space are described in terms of the Euler–Lagrange equation, but not with respect to the Lagrangian itself but with respect to the Routhian [15, 14, 12].

The 3D pendulum has a S^1 symmetry given by a rotation about the vertical axis. The symmetry action $\Phi_\theta : SO(3) \rightarrow SO(3)$ is given by

$$\Phi_\theta(R) = \exp(\theta\hat{e}_3)R,$$

for $\theta \in S^1$ and $R \in SO(3)$. It can be shown that the Lagrangian of the 3D pendulum is invariant under this symmetry action. Thus, the configuration space is reduced to the shape manifold $SO(3)/S^1 \cong S^2$, and the dynamics of the 3D pendulum is described in the tangent bundle TS^2 . This reduction procedure is interesting and challenging, since the projection $\Pi : SO(3) \rightarrow S^2$ given by $\Pi(R) = R^T e_3$ together with the symmetry action has a nontrivial principal bundle structure. In other words, the angle of the rotation about the vertical axis is not a global cyclic variable.

Here we present expressions for the Routhian and the reduced equations of motion. The detailed description and development can be found in the Appendix.

Proposition 15 ([15]). *We identify the Lie algebra of S^1 with \mathbb{R} . For $(R, \omega) \in T_R SO(3)$, the momentum map $\mathbf{J} : TSO(3) \rightarrow \mathbb{R}^*$, the locked inertia tensor $\mathbb{I}(R) : \mathbb{R} \rightarrow \mathbb{R}^*$, and the mechanical connection $\mathcal{A} : TSO(3) \rightarrow \mathbb{R}$ for the 3D pendulum are given as follows*

$$\mathbf{J}(R, \hat{\omega}) = e_3^T R J \omega, \quad (5.1)$$

$$\mathbb{I}(R) = e_3^T R J R^T e_3, \quad (5.2)$$

$$\mathcal{A}(R, \hat{\omega}) = \frac{e_3^T R J \omega}{e_3^T R J R^T e_3}. \quad (5.3)$$

The value of the momentum map $\mu = \mathbf{J}(R, \hat{\omega})$ corresponds to the vertical component of the angular momentum. Noether's theorem states that the symmetry of the Lagrangian implies conservation of the corresponding momentum map. This is an alternative method of showing the invariant properties of the 3D pendulum, as opposed to the direct computation used in Section 3.1.

Based on the above expressions, Lagrange–Routh reduction is carried out to obtain the following result.

Proposition 16. *For a given value of the momentum map μ , the Routhian of the 3D pendulum is given by*

$$R^\mu(\Gamma, \dot{\Gamma}) = \frac{1}{2}(\dot{\Gamma} \times \Gamma) \cdot J(\dot{\Gamma} \times \Gamma) - \frac{1}{2}(b^2 + \nu^2)(\Gamma \cdot J\Gamma) + mg\Gamma \cdot \rho, \quad (5.4)$$

where $b = \frac{J\Gamma \cdot (\dot{\Gamma} \times \Gamma)}{\Gamma \cdot J\Gamma}$, $\nu = \frac{\mu}{\Gamma \cdot J\Gamma}$, and the magnetic two form can be written as

$$\beta_\mu(\Gamma \times \eta, \Gamma \times \zeta) = -\frac{\mu}{(\Gamma \cdot J\Gamma)^2} \left[-(\Gamma \cdot J\Gamma)\text{tr}[J] + 2\|J\Gamma\|^2 \right] \Gamma \cdot (\eta \times \zeta). \quad (5.5)$$

The Routhian satisfies the Euler-Lagrange equation, with the magnetic term, given by

$$\delta \int_0^T R^\mu(\Gamma, \dot{\Gamma}) dt = \int_0^T \mathbf{i}_{\dot{\Gamma}} \beta_\mu(\delta\Gamma) dt. \quad (5.6)$$

This yields the reduced equation of motion on TS^2 :

$$\ddot{\Gamma} = -\|\dot{\Gamma}\|^2 \Gamma + \Gamma \times \Sigma, \quad (5.7)$$

where

$$\Sigma = b\dot{\Gamma} + J^{-1} \left[(J(\dot{\Gamma} \times \Gamma) - bJ\Gamma) \times ((\dot{\Gamma} \times \Gamma) - b\Gamma) + \nu^2 J\Gamma \times \Gamma - mg\Gamma \times \rho - c\dot{\Gamma} \right], \quad (5.8)$$

$$c = \nu \left\{ \text{tr}[J] - 2\frac{\|J\Gamma\|^2}{\Gamma \cdot J\Gamma} \right\}, \quad b = \frac{J\Gamma \cdot (\dot{\Gamma} \times \Gamma)}{\Gamma \cdot J\Gamma}, \quad \nu = \frac{\mu}{\Gamma \cdot J\Gamma}. \quad (5.9)$$

Proof. See the Appendix. □

5.2. Lagrange–Routh Reconstruction of the 3D pendulum. For a given value of the momentum map μ , let $\Gamma(t) \in S^2$ be a curve in the reduced space S^2 satisfying the Euler-Lagrange equation for the reduced Routhian R^μ given by (5.7). The reconstruction procedure is to find the curve $R(t) \in SO(3)$ in the configuration manifold that satisfies $\Pi(R(t)) = \Gamma(t)$ and $\mathbf{J}(R(t), R(t)^T \dot{R}(t)) = \mu$.

This is achieved in two steps. First, we choose any curve $R_{\text{hor}}(t) \in SO(3)$ in the configuration manifold such that its projection is equal to the reduced curve, i.e. $\Pi(R_{\text{hor}}(t)) = \Gamma(t)$. Now, the curve $R(t)$ can be written as $R(t) = \Phi_{\theta(t)}(R_{\text{hor}}(t))$ for some $\theta(t) \in S^1$. We find a differential equation for $\theta(t)$ so that the value of the momentum map for the reconstructed curve is conserved.

Proposition 17. *Suppose that the integral curve of the Lagrange–Routh reduced equation (5.7) is given by $(\Gamma(t), \dot{\Gamma}(t)) \in TS^2$, and the value of the momentum map μ is known. The following procedure reconstructs the motion of the 3D pendulum to obtain $(R(t), \omega(t)) \in TSO(3)$ such that $\Pi(R(t)) = \Gamma(t)$ and $\mathbf{J}(R(t), \omega(t)) = \mu$.*

1. Horizontally lift $\Gamma(t)$ to obtain $R_{\text{hor}}(t)$ by integrating the following equation with $R_{\text{hor}}(0) = R(0)$.

$$\dot{R}_{\text{hor}}(t) = R_{\text{hor}}(t)\hat{\omega}_{\text{hor}}(t), \quad (5.10)$$

where

$$\omega_{\text{hor}}(t) = \dot{\Gamma}(t) \times \Gamma(t) - b(t)\Gamma(t). \quad (5.11)$$

2. Determine $\theta_{\text{dyn}}(t) \in S^1$ by the following equation.

$$\theta_{\text{dyn}}(t) = \int_0^t \frac{\mu}{\Gamma(s) \cdot J\Gamma(s)} ds. \quad (5.12)$$

3. Reconstruct the curve in $T\text{SO}(3)$.

$$R(t) = \Phi_{\theta_{\text{dyn}}(t)}(R_{\text{hor}}(t)) = \exp[\theta_{\text{dyn}}(t)\hat{e}_3]R_{\text{hor}}(t), \quad (5.13)$$

$$\omega(t) = \omega_{\text{hor}}(t) + \nu(t)\Gamma(t). \quad (5.14)$$

Proof. See the Appendix. \square

This leads to the geometric phase formula that expresses the rotation angle about the vertical axis along a closed integral curve of the reduced equation.

Proposition 18. *Let $\Gamma(t)$ be a closed curve in S^2 , i.e. $\Gamma(0) = \Gamma(T)$ for some T . The geometric phase $\theta_{\text{geo}}(T) \in S^1$ of the 3D pendulum is defined by the relationship $R(T) = \Phi_{\theta_{\text{geo}}(T)}(R(0))$ when $\mu = 0$. This can be written as*

$$\theta_{\text{geo}}(T) = \int_{\mathcal{B}} \frac{2\|J\Gamma(t)\|^2 - \text{tr}[J](\Gamma(t) \cdot J\Gamma(t))}{(\Gamma(t) \cdot J\Gamma(t))^2} dA, \quad (5.15)$$

where \mathcal{B} is a surface in S^2 with $\Gamma(t)$ as boundary.

5.3. Invariants of the Lagrange–Routh Reduced Model. In this section we find an invariant of the motion for the Lagrange–Routh reduced model of the 3D pendulum, namely the total energy of the system. Note that the Lagrange–Routh reduced equations of motion are derived by elimination of the conserved vertical component of the body-fixed angular momentum. In later sections, we make use of the constant energy surfaces to understand the dynamics of the 3D pendulum.

Proposition 19. *The total energy*

$$E = \frac{1}{2}(\dot{\Gamma} \times \Gamma + (\nu - b)\Gamma)^T J(\dot{\Gamma} \times \Gamma + (\nu - b)\Gamma) - mg\rho^T \Gamma \quad (5.16)$$

is constant along motions of the Lagrange–Routh reduced equations for the 3D pendulum.

Proof. Substituting the reconstruction equations for the angular velocity (5.11), (5.14) into the total energy expression (4.6), we obtain (5.16). The time derivative of the total energy is given by

$$\dot{E} = (\dot{\Gamma} \times \Gamma + (\nu - b)\Gamma)^T J(\ddot{\Gamma} \times \Gamma + (\dot{\nu} - \dot{b})\Gamma + (\nu - b)\dot{\Gamma}) - mg\rho^T \dot{\Gamma}.$$

Substituting the reduced equation of motion (5.7) into the above equation and rearranging, we can show that $\dot{E} = 0$. \square

5.4. Equilibria of the Lagrange–Routh Reduced Model. The Lagrange–Routh reduced model can be considered as the Lagrange–Poincaré reduced model where the angular velocity is projected onto $T_{\Gamma}S^2$. Thus, the equilibria structure of the Lagrange–Routh reduced model is equivalent to the Lagrange–Poincaré reduced model, but it is represented by conditions on the reduced attitude Γ_e and the value of the momentum map μ instead of (Γ_e, ω_e) .

More explicitly, we study the equilibria structure of the Lagrange–Routh reduced model using (5.7), and we show it is equivalent to the families of equilibria presented in Proposition 9.

Proposition 20. *Consider the Lagrange–Routh reduced model of the 3D pendulum given by (5.7). The equilibria $(\Gamma_e, 0) \in T\text{SO}(3)$ of the Lagrange–Routh model are given for $\mu \in \mathbb{R}$ as follows.*

1. The hanging equilibrium: $\left(\frac{\rho}{\|\rho\|}, 0\right)$ $\mu = 0$,
2. The inverted equilibrium: $\left(-\frac{\rho}{\|\rho\|}, 0\right)$ $\mu = 0$,
3. Two relative equilibria:

$$\left(-\frac{J^{-1}\rho}{\|J^{-1}\rho\|}, 0\right) \quad \mu = \pm \sqrt{\frac{mg}{\|J^{-1}\rho\|^3}} \rho^T J^{-1}\rho, \quad (5.17)$$

4. One dimensional relative equilibrium manifolds:

$$\left(-\operatorname{sgn}(\alpha) \frac{n_\alpha}{\|n_\alpha\|}, 0 \right) \quad \mu = \pm \operatorname{sgn}(\alpha) \sqrt{\frac{mg}{\|n_\alpha\|^3}} n_\alpha^T J n_\alpha, \quad (5.18)$$

where $n_\alpha = (J - \frac{1}{\alpha} I_{3 \times 3})^{-1} \rho \in \mathbb{R}^3$ corresponding to $\alpha \in \mathcal{L}_i$, $i \in \{1, 2, 3, 4\}$ and

$$\mathcal{L}_1 = (-\infty, 0) \cup (\frac{1}{J_3}, \infty), \quad \mathcal{L}_2 = (0, \frac{1}{J_1}), \quad \mathcal{L}_3 = (\frac{1}{J_1}, \frac{1}{J_2}), \quad \mathcal{L}_4 = (\frac{1}{J_2}, \frac{1}{J_3}).$$

Also, $\operatorname{sgn}(\cdot)$ denotes the sign function.

The families of equilibria given in (5.18) converge to the hanging equilibrium and the inverted equilibrium when $\alpha \rightarrow 0$, and they converge to the third equilibria given in (5.17), when $\alpha \rightarrow \pm\infty$. If the vector from the pivot to the center of mass ρ , lies on a principal axis, i.e. $\rho \times e_i = 0$ for some $i \in \{1, 2, 3\}$, then (5.18) can be rewritten as $\{(e_i, 0), (-e_i, 0)\}$ for any $\mu \in \mathbb{R}$. Furthermore, there exist additional equilibria under the following assumptions on the moment of inertia matrix J and the vector from the pivot to the center of mass $\rho = [\rho_1 \ \rho_2 \ \rho_3]^T$.

5. J_1, J_2 and J_3 are distinct and $\rho_i = 0$. Then there exist one-dimensional relative equilibrium manifolds:

$$\left(-\frac{p_i}{\|p_i\|}, 0 \right) \quad \mu = \pm \sqrt{\frac{mg}{\|p_i\|^3}} p_i^T J p_i, \quad (5.19)$$

for $i \in \{1, 2, 3\}$, where $p_1 = (\gamma, \frac{\rho_2}{J_2 - J_1}, \frac{\rho_3}{J_3 - J_1})$, $p_2 = (\frac{\rho_1}{J_1 - J_2}, \gamma, \frac{\rho_3}{J_3 - J_2})$, $p_3 = (\frac{\rho_1}{J_1 - J_3}, \frac{\rho_2}{J_2 - J_3}, \gamma)$ and $\gamma \in \mathbb{R}$.

6. $J_1 = J_2 \neq J_3$.

(a) If $\rho_1 = \rho_2 = 0$. Then there exist two-dimensional relative equilibrium manifolds:

$$\left(-\frac{q}{\|q\|}, 0 \right) \quad \mu = \pm \sqrt{\frac{mg}{\|q\|^3}} q^T J q,$$

where $q = (\gamma, \delta, \frac{\rho_3}{J_3 - J_1})$ and $\gamma, \delta \in \mathbb{R}$.

(b) If $\rho_3 = 0$. Then there exist one-dimensional relative equilibrium manifolds:

$$\left(-\frac{r}{\|r\|}, 0 \right) \quad \mu = \pm \sqrt{\frac{mg}{\|r\|^3}} r^T J r,$$

where $r = (\frac{\rho_1}{J_1 - J_3}, \frac{\rho_2}{J_1 - J_3}, \gamma)$ and $\gamma \in \mathbb{R}$.

Proof. Substituting $\dot{\Gamma}_e = 0$ into (5.7)–(5.9), we obtain a condition for an equilibrium Γ_e for μ as

$$\Gamma_e \times J^{-1} [\nu^2 J \Gamma_e \times \Gamma_e - mg \Gamma_e \times \rho] = 0.$$

This is equivalent to

$$[\nu^2 J \Gamma_e \times \Gamma_e - mg \Gamma_e \times \rho] = k_2 J \Gamma_e \quad (5.20)$$

for a constant $k_2 \in \mathbb{R}$. Taking the dot product of this and Γ_e implies that $0 = k_2 \Gamma_e^T J \Gamma_e$. Since $\Gamma_e^T J \Gamma_e > 0$ as the moment of inertia matrix J is positive definite and $\Gamma_e \in S^2$, it follows that $k_2 = 0$. Thus, (5.20) is equivalent to

$$\nu^2 J \Gamma_e + mg \rho = k_1 \Gamma_e \quad (5.21)$$

for a constant $k_1 \in \mathbb{R}$. Note that this is equivalent to the equilibrium condition for the Lagrange-Poincaré reduced model given by (4.14): for any solution (Γ_e, k, k_1) of (4.14), we can choose μ such that $k^2 = \nu^2 = \frac{\mu^2}{(\Gamma_e^T J \Gamma_e)^2}$, which gives a solution of (5.21), and vice versa. Thus, the equilibria structure of the

Lagrange–Routh reduced model is equivalent to the equilibria of the Lagrange–Poincaré reduced model. For an equilibrium (Γ_e, ω_e) of the Lagrange–Poincaré reduced model, the value of the momentum map at the corresponding equilibrium of the Lagrange–Routh model is given by

$$\mu = k(\Gamma_e^T J\Gamma_e) = \omega_e^T \Gamma_e (\Gamma_e^T J\Gamma_e) \quad (5.22)$$

Substituting this into the equilibria presented in Proposition 9, we obtain the equilibria of the Lagrange–Routh reduced model. \square

5.5. Local Analysis of the Lagrange–Routh Reduced Model on TS^2 . We showed that in case $\mu = 0$, the Routh reduced model of the 3D pendulum has two isolated equilibria, namely the hanging equilibrium and the inverted equilibrium. These equilibria correspond to the disjoint equilibrium manifolds of the full equations of the 3D pendulum.

We next focused on these isolated equilibria of the Routh reduced equations. Using Proposition 20, the stability properties of the equilibrium manifolds of the 3D pendulum can be deduced by studying the Routh reduced equilibria for the case $\mu = 0$. Compared to the Lagrange–Poincaré reduced model, the Routh reduction procedure results in a set of complicated equations that are a challenge to analyze.

We now present local analyses of the Routh reduced model of the 3D pendulum near the hanging equilibrium and near the inverted equilibrium.

Consider the equations (3.22)–(3.24) representing the linearization of the full equations of motion of the 3D pendulum at the hanging equilibrium. It was shown before that the Lagrange–Poincaré reduced equations of motion can be written in terms of $(x_1, x_2, \dot{x}_1, \dot{x}_2, \dot{x}_3)$. As shown in Proposition 11, this result follows from the fact that any perturbation in $\Gamma \in S^2$ at Γ_h can be expressed in terms of $(x_1, x_2) \in \mathbb{R}^2$. In a similar fashion, one obtains the following result.

Proposition 21. *The linearization of the Routh reduced attitude dynamics of the 3D pendulum, at the equilibrium $(\Gamma_h, 0) = (R_e^T e_3, 0)$, described by equation (5.7) can be expressed using $(x_1, x_2, \dot{x}_1, \dot{x}_2) \in \mathbb{R}^4$ according to (3.22) and (3.23).*

Proof. In Proposition 11, it was shown that the perturbations in Γ at Γ_h can be described in terms of $(x_1, x_2) \in \mathbb{R}^2$. The proof then simply follows by noting that the equations of motion of the Routh reduced 3D pendulum is described in terms of $(\Gamma, \dot{\Gamma}) \in TS^2$. Thus the linearization of the Routh reduced 3D pendulum model can be described using $(x_1, x_2, \dot{x}_1, \dot{x}_2) \in \mathbb{R}^4$ according to (3.22) and (3.23). \square

The linearization of the Routh reduced attitude dynamics of the 3D pendulum, about the equilibrium $(0, \Gamma_h)$ is obtained from the linearized model of the full attitude dynamics by neglecting the dynamics corresponding to x_3 . Summarizing the above, the linearization of (5.7) about the hanging equilibrium $(0, \Gamma_h)$ is expressed as

$$\ddot{x}_1 + mgl_1 x_1 = 0, \quad (5.23)$$

$$\ddot{x}_2 + mgl_2 x_2 = 0. \quad (5.24)$$

It is clear that due to the presence of imaginary eigenvalues, stability of the hanging equilibrium $(\Gamma_h, 0)$ cannot be concluded. Therefore we next consider Lyapunov analysis.

Proposition 22. *The hanging equilibrium $(\Gamma_h, 0) = \left(\frac{\rho}{\|\rho\|}, 0\right)$ of the reduced dynamics of the 3D pendulum described by (5.7) is stable in the sense of Lyapunov.*

Proof. Consider the candidate Lyapunov function

$$V(\Gamma, \dot{\Gamma}) = \frac{1}{2}(\dot{\Gamma} \times \Gamma + (\nu - b)\Gamma)^T J(\dot{\Gamma} \times \Gamma + (\nu - b)\Gamma) + mg(\|\rho\| - \rho^T \Gamma). \quad (5.25)$$

Note that $V(\Gamma_h, 0) = 0$ and $V(\Gamma, \dot{\Gamma}) > 0$ elsewhere. Furthermore, the derivative along a solution of (4.3) and (4.4) is given by

$$\dot{V}(\Gamma, \dot{\Gamma}) = (\dot{\Gamma} \times \Gamma + (\nu - b)\Gamma)^T J(\ddot{\Gamma} \times \Gamma + (\dot{\nu} - \dot{b})\Gamma + (\nu - b)\dot{\Gamma}) - mg\rho^T \dot{\Gamma}.$$

Substituting the reduced equation of motion (5.7) into the above equation and rearranging, we can show that $\dot{V}(\Gamma, \dot{\Gamma}) = 0$. Thus, the hanging equilibrium of (5.7) is Lyapunov stable. \square

Remark 4. Note that combining Proposition 22 with Proposition 20 immediately yields the result in Proposition 2.

We next study the local properties of the Routh reduced equations of the 3D pendulum near the inverted equilibrium $(\Gamma_i, 0)$. Consider the linearization of (5.7) at an equilibrium $(\Gamma_i, 0) = (R_e^T e_3, 0)$, where $(R_e, 0)$ is an equilibrium of the inverted equilibrium manifold I. A result similar to Proposition 21 follows.

Proposition 23. *The linearization of the reduced attitude dynamics of the 3D pendulum, at the equilibrium $(\Gamma_i, 0) = (R_e^T e_3, 0)$, described by (5.7) can be expressed using $(x_1, x_2, \dot{x}_1, \dot{x}_2) \in \mathbb{R}^4$ according to (3.26) and (3.27).*

Summarizing the above, the linearization of (5.7) at the inverted equilibrium $(\Gamma_i, 0)$ is expressed as

$$\ddot{x}_1 - mgl_1 x_1 = 0, \quad (5.26)$$

$$\ddot{x}_2 - mgl_2 x_2 = 0. \quad (5.27)$$

Note that the linearization of (5.7) at the inverted equilibrium has two negative eigenvalues and two positive eigenvalues. Thus, the inverted equilibrium $(\Gamma_i, 0)$ of the Routh reduced model is unstable and locally there exists a two dimensional stable manifold and a two dimensional unstable manifold.

Proposition 24. *The inverted equilibrium $(\Gamma_i, 0) = \left(-\frac{\rho}{\|\rho\|}, 0\right)$ of the Routh reduced dynamics of the 3D pendulum described by (5.7) is unstable.*

Remark 5. Note that combining Proposition 24 with Proposition 20 immediately yields the result that the inverted equilibrium manifold I of the 3D pendulum given by (3.1)–(3.2) is unstable.

5.6. Poincaré Map on the Lagrange–Routh Reduced Model. A Poincaré map describes the evolution of intersection points of a trajectory with a transversal hypersurface of codimension one. Typically, one chooses a hyperplane, and considers a trajectory with initial conditions on the hyperplane. The points at which this trajectory returns to the hyperplane are then observed, which provides insight into the stability of periodic orbits or the global characteristics of the dynamics.

The Lagrange–Routh reduced equations for the 3D pendulum on TS^2 are a particularly suitable choice for analysis using a Poincaré map, since it has dimension 4. Since the total energy given by (5.16) is conserved, choosing a Poincaré section on TS^2 and restricting to an energy isosurface induces a Poincaré map on a 2-dimensional submanifold of TS^2 . We define a Poincaré section on TS^2 for the Lagrange–Routh dynamics of the 3D pendulum given by (5.7) as follows.

$$\mathcal{P} = \left\{ (\Gamma, \dot{\Gamma}) \in TS^2 \mid e_3^T \dot{\Gamma} = 0, e_3^T (\Gamma \times \dot{\Gamma}) > 0, \text{ and } E(\Gamma, \dot{\Gamma}) = \text{constant} \right\}.$$

Suppose $\Gamma \in \mathcal{P}$ is given. The tangent space $T_\Gamma S^2$ is a plane that is tangential to S^2 and perpendicular to Γ . The first condition of the Poincaré section, $e_3^T \dot{\Gamma} = 0$, determines a line in which the tangent vector $\dot{\Gamma} \in T_\Gamma S^2$ should lie, and the constraint of the total energy conservation fixes the magnitude of the tangent vector in that line. Thus, the tangent vector is uniquely determined up to sign change. The second condition of the Poincaré section resolves this ambiguity. It also excludes two reduced attitudes $\Gamma = \pm e_3$ for which the first condition is trivial; $e_3^T \dot{\Gamma} = 0$ for any $\dot{\Gamma} \in T_{e_3} S^2 \cup T_{-e_3} S^2$. Thus, \mathcal{P} can be equivalently identified as

$$\mathcal{P} = \left\{ \Gamma \in S^2 \mid e_3^T \dot{\Gamma} = 0, e_3^T (\Gamma \times \dot{\Gamma}) > 0, \text{ and } E(\Gamma, \dot{\Gamma}) = \text{constant} \right\},$$

where $(\Gamma, \dot{\Gamma})$ satisfies (5.7).

This Poincaré section in TS^2 is well-defined in the sense that for each element, the corresponding tangent vector is uniquely determined. The attitude and the angular velocity in $TSO(3)$ can be obtained by using the reconstruction procedure for the given value of the momentum map μ .

Fig. 5.1 shows particular examples for this Poincaré map. The pendulum body is chosen as an elliptic cylinder with properties of $m = 1$ kg, $J = \text{diag}[0.13, 0.28, 0.17]$ kgm², $\rho = [0, 0, 0.3]$ m. The initial condition are given by $R_0 = I_{3 \times 3}$ and $\omega_0 = c[1, 1, 1]$ rad/s, where the constant c is varied to give different total

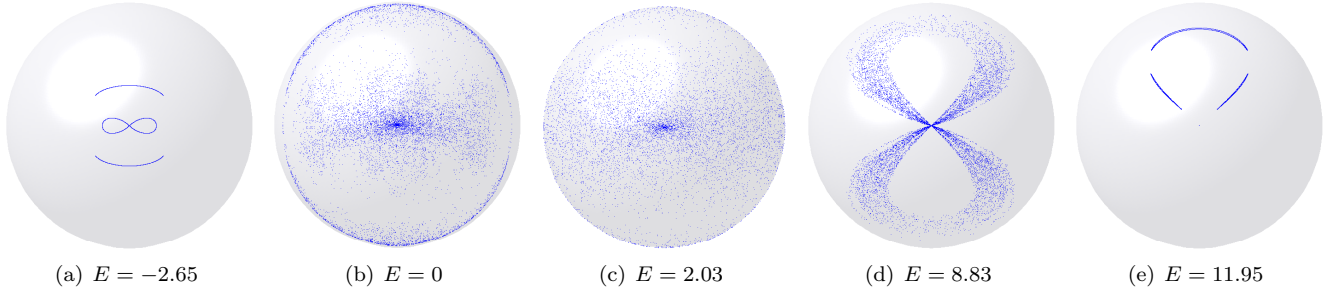


FIG. 5.1. Poincaré maps for 3D pendulum with varying total energy

energy levels. The Lie group variational integrator introduced in [13] is used to compute the Poincaré maps numerically.

It is interesting to see the transition of the Poincaré maps with varying total energy levels. The attitude dynamics of the 3D pendulum is periodic in Fig. 5.1(a), but it exhibits chaotic behavior with increased energy level in Fig. 5.1(b) and 5.1(c). If the total energy is increased further, the attitude dynamics becomes periodic again in Fig. 5.1(e). This demonstrates the highly-nonlinear, and perhaps chaotic, characteristics of the 3D pendulum dynamics.

6. Conclusions. The 3D pendulum exhibits rich dynamics with nontrivial geometric structure; these dynamics are much richer and more complex than the dynamics of a 1D planar pendulum or a 2D spherical pendulum. This paper has demonstrated that the methods of geometric mechanics and the methods of nonlinear dynamics can be meshed to obtain insight into the complex dynamics of the 3D pendulum.

We have introduced three different models of the 3D pendulum, including the full model defined on $TSO(3)$, the Lagrange–Poincaré reduced model on $TSO(3)/S^1$ obtained by identifying configurations in the same group orbit, and the Lagrange–Routh reduced model on TS^2 where one additionally utilizes the fact that the dynamics evolves on a momentum level set. Relationships between the various representations are discussed in the context of conservation properties, equilibria and their stability properties, and invariant manifolds.

In addition, we illustrate that the use of the Lagrange–Routh reduced equations of motion, together with the energy conservation properties, allow the construction of a Poincaré map that can be readily visualized, thereby providing a graphical tool for obtaining insight into the rich nonlinear dynamical properties of the 3D pendulum.

Appendix.

In this appendix, we summarize Lagrange–Routh reduction and reconstruction procedures for the 3D pendulum.

A.1. Reduction. A description of Lagrange–Routh reduction can be found in [15] including expressions for the mechanical connection and the Routhian of the 3D pendulum given by (5.3) and (5.4), respectively. Here we derive the reduced equation of motion (5.7) using the Euler–Lagrange equation for the given Routhian (5.4).

Variation of Routhian. The Routhian satisfies the variational Euler–Lagrange equation with the magnetic term given by (5.6). We use constrained variations of $\Gamma \in S^2$:

$$\delta\Gamma = \Gamma \times \eta, \quad (\text{A.1})$$

$$\delta\dot{\Gamma} = \dot{\Gamma} \times \eta + \Gamma \times \dot{\eta}. \quad (\text{A.2})$$

Here we assume that $\eta \cdot \Gamma = 0$, since the component of η parallel to Γ has no effect on $\delta\Gamma$. These expressions are essential for developing the reduced equation of motion.

Using (A.1), (A.2), and the properties $\Gamma \cdot \dot{\Gamma} = 0$, $\Gamma \cdot \eta = 0$, the variation of the Routhian is given by

$$\delta R^\mu = \dot{\eta} \cdot J(\dot{\Gamma} \times \Gamma - b\Gamma) - \eta \cdot \Gamma \times \left[-\dot{\Gamma} \times J(\dot{\Gamma} \times \Gamma) + (b^2 + \nu^2)J\Gamma - bJ(\dot{\Gamma} \times \Gamma) + b(\dot{\Gamma} \times J\Gamma) + mg\rho \right]. \quad (\text{A.3})$$

Magnetic 2-form. From the given mechanical connection \mathcal{A} and a value of the momentum map $\mu \in \mathbb{R}^*$, define a 1-form \mathcal{A}_μ on $TSO(3)$ by

$$\mathcal{A}_\mu(R) \cdot (R, \hat{\omega}) = \langle \mu, \mathcal{A}(R, \hat{\omega}) \rangle = \mu \frac{e_3^T R J \omega}{e_3^T R J R^T e_3}$$

The magnetic 2-form β_μ in (5.5) is the exterior derivative of \mathcal{A}_μ , which can be obtained by using the identity $\mathbf{d}\mathcal{A}_\mu(X, Y) = X[\mathcal{A}_\mu(Y)] - Y[\mathcal{A}_\mu(X)] - \mathcal{A}_\mu([X, Y])$ for $X = R\hat{\eta}$, $Y = R\hat{\zeta} \in T_R SO(3)$. Suppose that $\dot{\Gamma} = \Gamma \times \omega$. Since $\Gamma \cdot (\omega \times \eta) = \eta \cdot (\Gamma \times \omega) = \eta \cdot \dot{\Gamma}$, the interior product of the magnetic 2-form is given by

$$\mathbf{i}_{\dot{\Gamma}} \beta_\mu(\delta\Gamma) = \beta_\mu(\Gamma \times \omega, \Gamma \times \eta) = \nu \left\{ \text{tr}[J] - 2 \frac{\|J\Gamma\|^2}{\Gamma \cdot J\Gamma} \right\} \dot{\Gamma} \cdot \eta, \quad (\text{A.4})$$

where $\nu = \frac{\mu}{\Gamma \cdot J\Gamma}$.

Euler-Lagrange equation with magnetic 2-form. Substituting (A.3) and (A.4) into (5.6), and integrating by parts, the Euler-Lagrange equation for the reduced Routhian (5.4) is written as

$$-\int_0^T \eta \cdot \left[J(\ddot{\Gamma} \times \Gamma - b\dot{\Gamma} - \dot{b}\Gamma) + \Gamma \times X + c\dot{\Gamma} \right] dt = 0, \quad (\text{A.5})$$

where

$$X = -\dot{\Gamma} \times J(\dot{\Gamma} \times \Gamma) + (b^2 + \nu^2)J\Gamma - bJ(\dot{\Gamma} \times \Gamma) + b(\dot{\Gamma} \times J\Gamma) + mg\rho, \quad (\text{A.6})$$

and c is given by (5.9). Since (A.5) is satisfied for all η with $\Gamma \cdot \eta = 0$, we obtain

$$J(\ddot{\Gamma} \times \Gamma - b\dot{\Gamma} - \dot{b}\Gamma) + \Gamma \times X + c\dot{\Gamma} = \lambda\Gamma, \quad (\text{A.7})$$

for $\lambda \in \mathbb{R}$. This is the reduced equation of motion. However, this equation has an ambiguity since the value of λ is unknown; this equation is implicit for $\ddot{\Gamma}$ since the term \dot{b} is expressed in terms of $\ddot{\Gamma}$. The next step is to determine expressions for λ and \dot{b} using the definition of b and some vector identities.

We first find an expression for λ in terms of $\Gamma, \dot{\Gamma}$. Taking the dot product of (A.7) with Γ , we obtain

$$\Gamma \cdot J(\ddot{\Gamma} \times \Gamma - b\dot{\Gamma} - \dot{b}\Gamma) = \lambda. \quad (\text{A.8})$$

From the definition of b , we can show the following identity: $\Gamma \cdot J(\dot{\Gamma} \times \Gamma - b\Gamma) = 0$. Differentiating this with time, and substituting into (A.8), we find an expression for λ in terms of $\Gamma, \dot{\Gamma}$ as

$$\lambda = -\dot{\Gamma} \cdot J(\dot{\Gamma} \times \Gamma - b\Gamma). \quad (\text{A.9})$$

Substituting (A.9) into (A.7), and taking the dot product of the result with Γ , we obtain an expression for \dot{b} in terms of $\Gamma, \dot{\Gamma}$ as

$$\dot{b} = \Gamma \cdot J^{-1} \left\{ \Gamma \times X + c\dot{\Gamma} + (\dot{\Gamma} \cdot J(\dot{\Gamma} \times \Gamma - b\Gamma))\Gamma \right\}. \quad (\text{A.10})$$

Substituting (A.10) into (A.7), and using the vector identity $Y - (\Gamma \cdot Y)\Gamma = (\Gamma \cdot \Gamma)Y - (\Gamma \cdot Y)\Gamma = -\Gamma \times (\Gamma \times Y)$ for any $Y \in \mathbb{R}^3$, we obtain the following form for the reduced equation of motion

$$\ddot{\Gamma} \times \Gamma - b\dot{\Gamma} - \Gamma \times \left[\Gamma \times J^{-1} \left\{ \Gamma \times X + c\dot{\Gamma} + (\dot{\Gamma} \cdot J(\dot{\Gamma} \times \Gamma - b\Gamma))\Gamma \right\} \right] = 0.$$

Reduced equation of motion. This equation has no ambiguity. Now, we simplify this equation. The above expression is equivalent to the following equation

$$\Gamma \times \left[\ddot{\tilde{\Gamma}} \times \Gamma - b\dot{\tilde{\Gamma}} - \Gamma \times \left[\Gamma \times J^{-1} \left\{ \Gamma \times X + c\dot{\tilde{\Gamma}} + (\dot{\tilde{\Gamma}} \cdot J(\dot{\tilde{\Gamma}} \times \Gamma - b\Gamma))\Gamma \right\} \right] \right] = 0.$$

Since $\Gamma \cdot \ddot{\tilde{\Gamma}} = -\|\dot{\tilde{\Gamma}}\|^2$, the first term is given by

$$\Gamma \times (\ddot{\tilde{\Gamma}} \times \Gamma) = (\Gamma \cdot \Gamma)\ddot{\tilde{\Gamma}} - (\Gamma \cdot \ddot{\tilde{\Gamma}})\Gamma = \ddot{\tilde{\Gamma}} + \|\dot{\tilde{\Gamma}}\|^2\Gamma.$$

Using the property $\Gamma \times (\Gamma \times (\tilde{\Gamma} \times Y)) = -(\Gamma \cdot \Gamma)\Gamma \times Y = -\Gamma \times Y$ for $Y \in \mathbb{R}^3$, the third term of the above equation can be simplified. Substituting (A.6) and rearranging, the reduced equation of motion for the 3D pendulum is given by

$$\ddot{\tilde{\Gamma}} = -\|\dot{\tilde{\Gamma}}\|^2\Gamma + \Gamma \times \Sigma, \quad (\text{A.11})$$

where $\Sigma = b\dot{\tilde{\Gamma}} + J^{-1} \left[(J(\dot{\tilde{\Gamma}} \times \Gamma) - bJ\Gamma) \times ((\dot{\tilde{\Gamma}} \times \Gamma) - b\Gamma) + \nu^2 J\Gamma \times \Gamma - mg\Gamma \times \rho - c\dot{\tilde{\Gamma}} \right]$.

A.2. Reconstruction. For a given integral curve of the reduced equation $(\Gamma(t), \dot{\tilde{\Gamma}}(t)) \in TS^2$, we find a curve $\tilde{R}(t) \in SO(3)$ that is projected into the reduced curve, i.e. $\Pi(\tilde{R}(t)) = \Gamma(t)$. The reconstructed curve can be written as $R(t) = \Phi_{\theta(t)}(\tilde{R}(t))$ for some $\theta(t) \in S^1$. The conservation of the momentum map yields the following reconstruction equation [15].

$$\theta(t)^{-1}\dot{\theta}(t) = \mathbb{I}^{-1}(\tilde{R}(t))\mu - \mathcal{A}(\dot{\tilde{R}}(t)).$$

The particular choice of $\tilde{R}(t)$, the horizontal lift given by (5.10), simplifies the above equation, since the horizontal part of the tangent vector is annihilated by the mechanical connection. Further, since the group S^1 is abelian, the solution reduces to a quadrature such as (5.12). The reconstructed curve is given by (5.13).

REFERENCES

- [1] K. J. ASTROM AND K. FURUTA, *Swinging up a pendulum by energy control*, Automatica, 36 (2000), pp. 287–295.
- [2] R. E. BELLMAN, *Introduction to Matrix Analysis*, Society for Industrial and Applied Mathematics, 2nd ed., 1997.
- [3] D. S. BERNSTEIN, *Matrix Mathematics, Theory, Facts, and Formulas with Applications to Linear System Theory*, Princeton University Press, 2005.
- [4] D. S. BERNSTEIN, N. H. MCCLAMROCH, AND A. M. BLOCH, *Development of air spindle and triaxial air bearing testbeds for spacecraft dynamics and control experiments*, Proceedings of the American Control Conference, (2001), pp. 3967–3972.
- [5] A. M. BLOCH, *Nonholonomic Mechanics and Control*, Springer-Verlag, 2003.
- [6] H. CENDRA, J. E. MARSDEN, AND T. S. RATIU, *Lagrangian reduction by stages*, Mem. Amer. Math. Soc., 152 (2001).
- [7] N. A. CHATURVEDI AND N. H. MCCLAMROCH, *Asymptotic stabilization of the hanging equilibrium manifold of the 3D pendulum*. submitted, 2006.
- [8] S. CHO, J. SHEN, AND N. H. MCCLAMROCH, *Mathematical models for the triaxial attitude control testbed*, Mathematical and Computer Modeling of Dynamical Systems, 9 (2003), pp. 165–192.
- [9] S. CHO, J. SHEN, N. H. MCCLAMROCH, AND D. S. BERNSTEIN, *Equations of motion of the triaxial attitude control testbed*, Proceedings of the IEEE Conference on Decision and Control, (2001), pp. 3429–3434.
- [10] K. FURUTA, *Control of pendulum: From super mechano-system to human adaptive mechatronics*, Proceedings of the IEEE Conference on Decision and Control, (2003), pp. 1498–1507.
- [11] A. HERNÁNDEZ-GARDUÑO, J. K. LAWSON, AND J. E. MARSDEN, *Relative equilibria for the generalized rigid body*, Journal of Geometry and Physics, 53 (2005), pp. 259–274.
- [12] P. J. HOLMES AND J. E. MARSDEN, *Horseshoes and Arnol diffusion for Hamiltonian systems on Lie groups*, Indiana U. Math. Journal, 32 (1983), pp. 962–967.
- [13] T. LEE, M. LEOK, AND N. H. MCCLAMROCH, *A lie group variational integrator for the attitude dynamics of a rigid body with application to the 3D pendulum*, Proceedings of the IEEE Conference on Decision and Control, (2005), pp. 962–967.
- [14] D. LEWIS, T. S. RATIU, J. C. SIMO, AND J. E. MARSDEN, *The heavy top: A geometric treatment*, Nonlinearity, 5 (1992), pp. 1–48.
- [15] J. E. MARSDEN, T. S. RATIU, AND J. SCHEURLE, *Reduction theory and the lagrange-routh equations*, Journal of Mathematical Physics, 41 (2000), pp. 3379–3429.
- [16] J. SHEN, A. K. SANYAL, N. A. CHATURVEDI, D. S. BERNSTEIN, AND N. H. MCCLAMROCH, *Dynamics and control of a 3D pendulum*, Proceedings of the IEEE Conference on Decision and Control, (2004), pp. 323–328.